International Journal of General Medicine

Dovepress
open access to scientific and medical research

Open Access Full Text Article

ORIGINAL RESEARCH

Diagnostic Value of CT Delayed Phase Images Added to Gd-EOB-DTPA MRI for HCC Diagnosis in LR-3/4 Lesions

Zhang Qing, Huang Yuan, Xiong Hao, Peng Jie

Department of Radiology, Jingzhou No 1 People's Hospital and First Affiliated Hospital of Yangtze University, Jingzhou City, Hubei Province, 434000, People's Republic of China

Correspondence: Peng Jie, Department of Radiology, The Jingzhou No 1 People's Hospital and First Affiliated Hospital of Yangtze University, Hangkong Road, Shashi District, Jingzhou City, Hubei Province, 434000, People's Republic of China, Tel +86 181 6313 1595, Email 18163131595vip@sina.com

Objective: To explore the potential value of gadolinium-ethoxybenzyl-diethylenetriamine pentaacetic acid (Gd-EOB-DTPA) magnetic resonance imaging (MRI) in the diagnosis of hepatocellular carcinoma (HCC) in LR-3/4 lesions by adding computed tomography (CT) delayed images based on the Liver Imaging Reporting And Data System (LI-RADS).

Methods: The differences in clinical and imaging characteristics between hepatocellular carcinoma and non-HCC were compared, and logistic regression was used to analyze the imaging risk factors for the diagnosis of HCC. Based on the main and HCC-specific auxiliary features of Gd-EOB-DTPA MRI, the HCC diagnostic model 1 was established, and the diagnostic efficacy was analyzed. Based on model 1, delayed phase CT images were added to establish model 2 to find reliable predictors of HCC diagnosis. Receiver operating characteristic (ROC) analysis and the DeLong test were used to compare the two models.

Results: There was a significant difference in serum AFP between HCC and non-HCC ($P = 0.008$). Based on main and HCC-specific auxiliary features of Gd-EOB-DTPA MRI, enhancing capsule (OR = 0.197, 95% CI = 0.06–0.595, $P = 0.005$) and washout (OR = 10.345, 95% CI = 3.460–30.930, $P < 0.001$) were independent risk factors in Model 1. After adding CT delayed-phase images to build model 2, enhancing capsule (OR = 0.132, 95% CI = 0.139–0.449, $P = 0.001$), MRI and (or) CT washout (OR = 0.052, 95% CI = 0.016–0.172, $P < 0.001$) were reliable predictors for HCC diagnosis. The AUC of model 1 was 0.808, sensitivity was 63.46%, and specificity was 85.00%. The AUC of model 2 was 0.854, the sensitivity was 71.20%, and the specificity was 85.00%. DeLong test ($P = 0.040$) demonstrated the diagnostic efficacy of model 2 significantly superior than model 1.

Conclusion: Tumor washout and enhanced capsule are reliable factors for the diagnosis of HCC. Gd-EOB-DTPA MRI with delayed phase CT images can improve the sensitivity and diagnostic efficiency of HCC in LR-3/4 lesions on the premise of maintaining high specificity. Future studies are required to reinforce our finding.

Keywords: liver imaging reporting and data system, gadolinium-ethoxybenzyl-diethylenetriamine pentaacetic acid, computed tomography, hepatocellular carcinoma, diagnostic performance

Introduction

Hepatocellular carcinoma (HCC) is a major contributor to the world's cancer burden and incidence rates have increased in many countries in recent decades, and it is the second most prevalent malignancy, 300,000 to 400,000 people die from it every year in China where it has the greatest number of cases, due to both an elevated rate (18.3 per 100,000) and the world's largest population.[1–3] Imaging examinations, especially computed tomography (CT) and magnetic resonance imaging (MRI), play a crucial role in the diagnosis of HCC.[4] The Liver Imaging Reporting And Data System (LI-RADS) standardizes the collection, interpretation and reporting of liver lesions in high-risk HCC patients, aiming to improve the diagnostic efficacy of imaging in high-risk HCC patients.[5,6] However, it is still uncertain whether and how the technical difference between CT and MRI will affect the imaging observations and the final scoring results of LI-RADS, and whether these imaging features from different technologies can be integrated into a single widely accepted diagnostic algorithm to improve diagnostic performance.

Received: 16 March 2023
Accepted: 31 May 2023
Published: 12 June 2023

Gadolinium-ethoxybenzyl-diethylenetriamine pentaacetic acid (Gd-EOB-DTPA) is a hepatocyte-specific MR contrast agent, which can provide information on hepatic hemodynamics and hepatic function. Gd-EOB-DTPA makes the early diagnosis of HCC possible and improves the diagnostic efficiency.[7–10] For patients with high risk of liver tumor, EOB-MRI is the first recommended imaging examination. However, due to the uptake of contrast agents by normal hepatocytes, the transitional phase of Gd-EOB-DTPA contrast-enhanced imaging and delayed phase of extracellular contrast-enhanced imaging are different. According to the current version of LI-RADS, washout should only be evaluated in the portal phase for Gd-EOB-DTPA contrast-enhanced MRI to maintain high specificity under the premise of sacrificing some sensitivity.[11,12] Some lesions, however, only showed washout in the delayed phase, and defining washout only during the portal phase may lead to missed diagnosis or downgrading of tumor LI-RADS due to lower sensitivity.[13,14] Further characterization and differentiation of these lesions requires the application of ancillary imaging features, acquisition of specific MRI sequences, or the application of CT, which can provide further information concerning their cellularity, function, and vascularity.

According to previous research, there is a concern about lowering specificity as a trade-off for increasing sensitivity when using hepatobiliary phase defining washout.[15] Although sensitivity can be improved without reducing specificity by extending washout appearance to the transitional or hepatobiliary phase, it comes at the cost of false positives, and only after excluding hemangiomas and non-HCC malignancies.[16] Enhanced CT can show the washout of HCC as it provides information about hepatic hemodynamics. CT examination is one of the most commonly used methods for the screening and preliminary diagnosis of liver or epigastric lesions, and many patients have undergone CT before the EOB. Based on the above theoretical and practical basis, the purpose of this study is to explore the potential value of Gd-EOB-DTPA MRI by adding CT delayed phase images in the diagnosis of HCC based on LI-RADS.

Methods and Materials

Study Population

The ethics committee of Jingzhou No 1 People's Hospital waived the need for specific patient informed consent due to the retrospective nature of the study, and the data was anonymized or maintained with confidentiality. All methods were performed in accordance with the Declaration of Helsinki. From November 2017 to November 2020, patients with suspected liver or epigastric lesions who underwent enhanced CT in our hospital were collected, and those who underwent Gd-EOB-DTPA MRI because of high-risk factors for HCC were selected. All clinicopathological information was obtained through the medical record system of our hospital. The inclusion criteria were (a) Enhanced CT was performed within 2 weeks before Gd-EOB-DTPA enhancement in our hospital; (b) According to LI-RADS v2018, the lesions were classified as LR-3, 4; (c) Complete pathological or follow-up results were available. The exclusion criteria were (a) The patient had a history of liver tumor radiofrequency ablation (RFA), transcatheter arterial chemoembolization (TACE), targeted therapy, or systemic chemotherapy before CT and MRI examination; (b) The lesion was confirmed to be malignant for enlargement or metastasis rather than pathological confirmation during the follow-up; (c) Image quality was not good enough to meet diagnostic requirements. Detailed information about the patient selection procedure is presented in Figure 1.

CT and MRI Technique

Gemstone spectral CT (GE Discovery HD750 CT) was used to scan the liver. The scanning parameters were tube voltage 120 kVp, tube current 120 mAs, slice thickness 5mm, thin slice 0.625 mm, slice spacing 5mm. Then, 100 mL iohexol was injected through the elbow vein at the injection rate of 3 mL/s. Dynamic contrast-enhanced scan was performed, including arterial phase (AP, 30s), portal vein phase (PVP, 60s) and delayed phase (DP, 120s).

MR Imaging of the liver was performed on a Philips 3.0T MR System (Intera Achieva TX). Scanning sequence and parameters: Conventional T1-weighted imaging (T1WI) axial, fat-suppression T2-weighted imaging (T2WI) axial, coronal T2WI, using gradient echo sequence DWI (b = 50s/mm^2, 800s/mm^2) axial scan, TR 4.154ms, TE 2.20ms, matrix 154 × 192, slice thickness 5.5mm, slice spacing 1.0mm. The field of view was 260mm × 260mm. A rapid bolus of Gd-EOB-DTPA was administered via the cubital vein at a contrast dose of 0.1 mL/kg body weight at an injection rate of

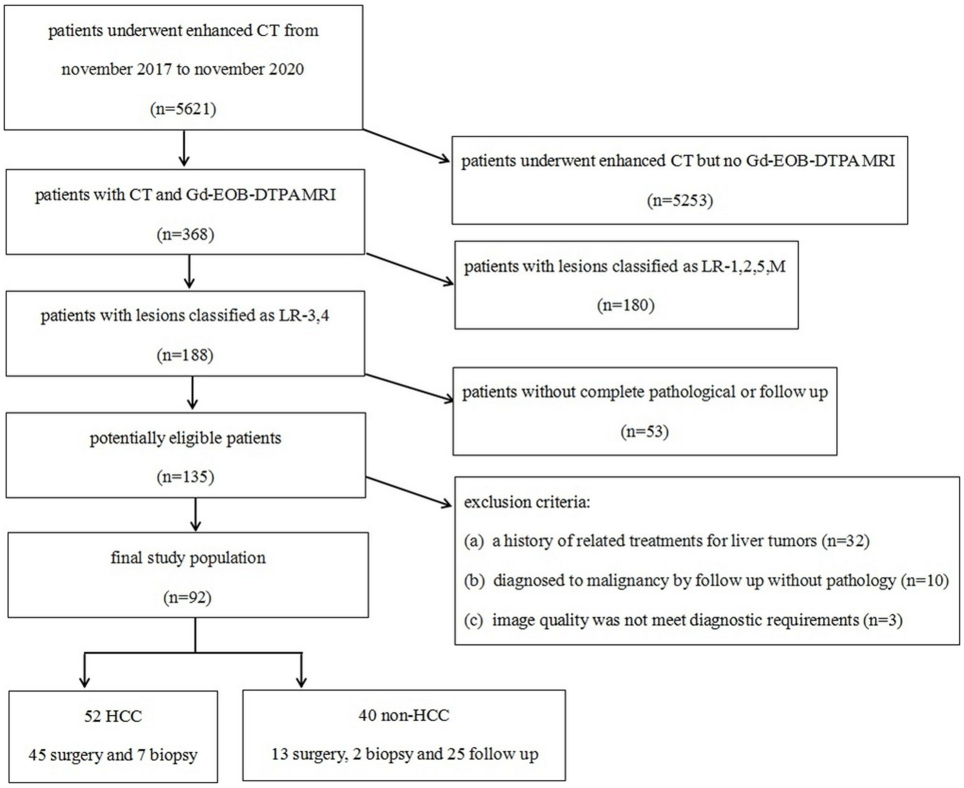

Figure 1 Flowchart of the inclusion and exclusion criteria.

1.0 to 1.5 mL/s, followed by flushing with 20 mL of normal saline using a high-pressure syringe. Dynamic imaging was performed using enhanced-T1 high resolution isotropic volume examination (e-THRIVE), including arterial phase (AP, 20–25 s), portal venous phase (PVP, 60–70s), transition phase (TP, 2 min) and hepatobiliary phase (HBP, 20 min).

Image Analysis

The imaging features were analyzed by two experienced abdominal radiologists (with 7 and 20 years of experience in CT and MRI, respectively) independently, who were blinded to the pathological diagnosis and from each other's findings. Among the patients with multiple lesions, only the largest one was analyzed. According to LI-RADS v2018 standard and Gd-EOB-DTPA features, LR-3 and 4 patients were selected, and the presence or absence of main MRI features and HCC-specific auxiliary features were analyzed. Based on delayed phase images of CT, defining CT washout appearance. Any discrepancies were resolved by consensus.

Reference Imaging Features

The following features were evaluated based on LI-RADS v2018.[12] Major features: a) nonrim arterial phase hyperenhancement (APHE); b) nonperipheral washout; c) enhancing capsule. HCC-specific auxiliary features: a) nonenhancing capsule; b) nodule-in-nodule architecture; c) mosaic architecture; d) fat in mass; e) blood products in mass.

Statistical Analysis

Statistical analysis was performed using SPSS (Solutions statistical Package For The Social Sciences, IBM Corporation, Armonk, NY) version 24.0 and MedCalc 20.0.14. All parameters were assessed by intraclass correlation coefficient (ICC), with $k > 0.75$ were statistically analyzed. Continuous variables were performed using the Student's *t*-test or the Mann–Whitney *U*-test. Categorical variables were compared using the Chi-squared or Fisher's exact test. Multivariable logistic regression analysis was used to identify the imaging risk factors for the diagnosis of HCC. Gd-EOB-DTPA MRI features with $P < 0.05$ in univariate analysis were included in multivariate logistic regression analysis to establish the

HCC diagnostic model 1. Then, diagnostic model 2 was established by adding CT delay phase features to model 1 to find reliable predictors of HCC diagnosis. The receiver operating characteristic (ROC) curve analysis was performed with sensitivity, specificity, and area under the receiver operating curve (AUC) to evaluate the diagnostic efficacy of the two models. DeLong test was used to compare the two models. The statistical significance was considered when $P < 0.05$.

Results

Patient Characteristics and Pathologic Findings

Eligible LR-3,4 patients were selected according to the LI-RADS v2018. All 52 cases of HCC were confirmed by surgery or biopsy pathology. Fifteen cases of non-HCC were confirmed by surgery or biopsy pathology, including 5 cases of Intrahepatic cholangiocarcinoma (ICC), 2 cases of mixed HCC-ICC, 4 cases of inflammatory myofibroblastic tumor, 2 cases of hepatic adenoma, and 2 cases of focal nodular hyperplasia. All pathological findings were obtained within 1 month after MRI examination. Ten cases were excluded, which were confirmed to be malignant by enlargement or metastasis of the lesion during follow-up but without definite pathology. Twenty-five cases with no change after more than 2 years of follow-up were included in the non-HCC group. In total, there were 52 cases in the HCC group and 40 cases in the non-HCC group, 45 cases in LR-4, and 47 cases in LR-3. The comparison of clinical characteristics between the two groups is shown in Table 1.

LI-RADS Features of Tumors

Representative cases of HCC are shown in Figures 2 and 3. The imaging features and consistency evaluation of LI-RADS are shown in Table 2. The consistency of image features between the two observers was good ($k \geq 0.776$). Seventy-one percent of patients had APHE in the arterial phase. Forty-two percent of patients showed washout in Gd-EOB-DTPA MRI, and 48% of patients showed washout in CT delayed phase. All patients with MRI washout in PVP were found in CT delayed phase. In addition, 4 cases of HCC showed no washout in Gd-EOB-DTPA MRI, but washout in CT delayed phase. One case of mixed HCC-ICC showed no washout in Gd-EOB-DTPA MRI, but washout in CT delayed phase.

Logistic Regression Analysis and Diagnostic Performance of HCC

Logistic regression analysis results are shown in Table 3. Based on Gd-EOB-DTPA MRI, washout (*OR* = 10.345, 95% CI = 3.460–30.930, P < 0.001), enhancing capsule (OR = 0.197, 95% CI = 0.065–0.595, P = 0.004) were independent risk factors for HCC in Model 1. AUC = 0.808, sensitivity = 63.46%, specificity = 85.00%, positive predictive value (PPV) = 84.60%, negative predictive value (NPV) = 64.20%, and accuracy = 72.80% for model 1.

After adding CT delayed phase imaging features, Gd-EOB-DTPA MRI and (or) CT delayed phase washout (*OR* = 0.052, 95% CI = 0.016–0.172, *P* < 0.001), enhancing capsule (*OR* = 0.132, 95% CI = 0.139–0.449, *P* = 0.001) were

Table 1 Characteristics of the Study Population

Variable	HCC (n = 52)	Non-HCC (n = 40)	*P* value
Age (year)	56.4±9.2	55.9±8.3	0.414
Gender(Male/Female)	34/18	26/14	0.571
Cirrhosis	30	24	0.497
HBV	36	22	0.118
HCV	3	2	0.624
Alcoholic	5	3	0.512
Child-Pugh A/B /C	38/10/4	29/8/3	0.996
Diameter(cm)	3.1±1.4	2.6±1.8	0.192
AFP(≥20.0 ng/mL)	26	9	0.008*

Note: *Values with statistical difference.
Abbreviations: HBV, Hepatitis B viral; HCV, Hepatitis C viral; AFP, α-fetoprotein; HCC, hepatocellular carcinoma.

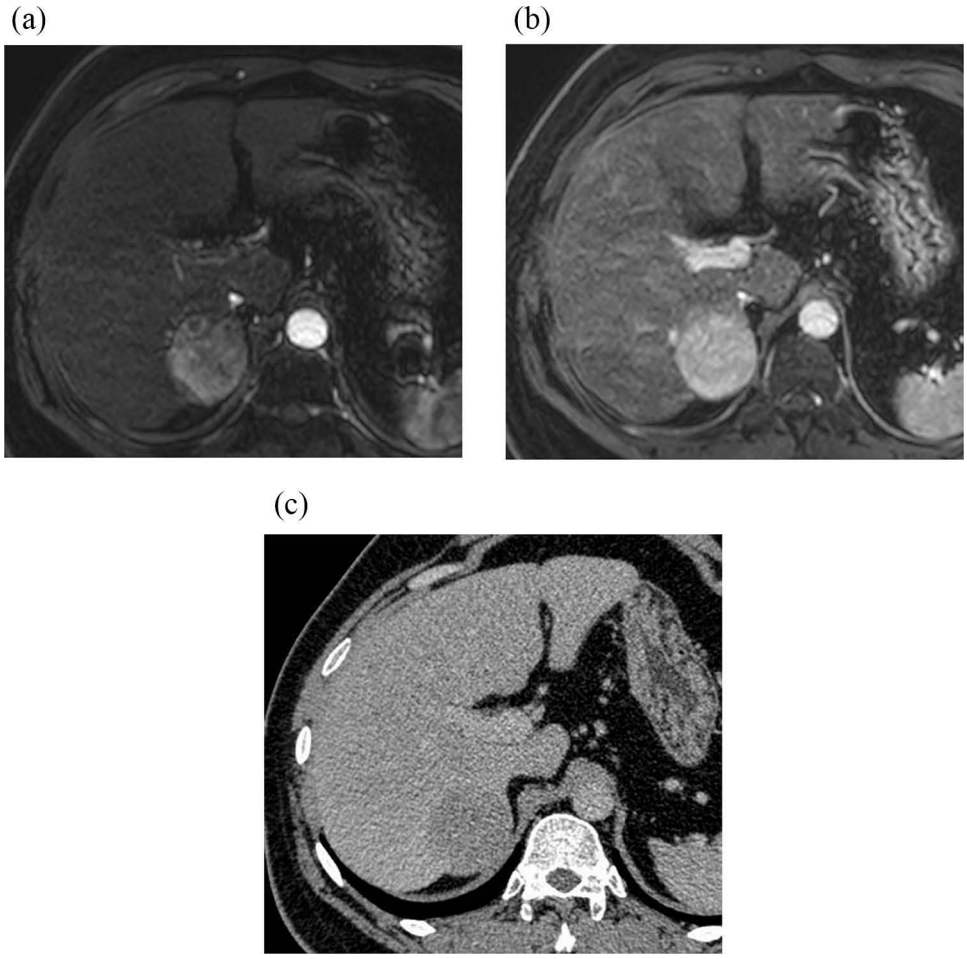

Figure 2 56-year-old man with cirrhosis and HCC. (**a**) APHE of Gd-EOB-DTPA MRI. Figure (**b**) shows no washout and no capsule in PVP of Gd-EOB-DTPA MRI. Tumor diameter > 2cm, and LR-4. Figure (**c**) shows washout in delayed phase of CT. Adding CT delayed phase images to Gd-EOB-DTPA MRI, the lesion was classified as LR-5.

independent risk factors for predicting HCC in Model 2. AUC = 0.854, sensitivity = 71.20%, specificity = 85.00%, PPV = 78.00%, NPV = 81.80%, and accuracy = 79.30% for model 2.

Model 2 demonstrated significantly superior AUC (0.854 vs 0.808), and sensitivity (71.20% vs 63.46%) compared with Model 1 according to DeLong test ($P = 0.040$) (Figure 4). In general, adding CT delayed phase images resulted in significant improvements in diagnostic performance.

Disscusion

LI-RADS solves the problem of standardized diagnosis of HCC to a certain extent and can make a definite diagnosis of LR-5 lesions. However, accurate diagnosis of LR-3 and LR-4 lesions is still a challenge. Gd-EOB-DTPA MRI has been gradually popularized and has become an important imaging method for high-risk patients with HCC due to high diagnostic efficiency.[17] Therefore, we aimed to study patients in LR-3, 4 of LI-RADS in the context of Gd-EOB-DTPA MRI. Recent studies using Gd-EOB-DTPA-enhanced MRI based on LI-RADS have shown high specificity (>88%) despite low sensitivity (60.5–75%).[18–20] The specificity of our results was slightly lower (85%), presumably because our sample excluded LR-5 patients with a definite HCC diagnosis, for which Gd-EOB-DTPA enhancement has particularly high specificity. The results of this study showed that the image features of the two readers had a high consistency, which was consistent with the literature reports.[21,22]

In our study, washout and enhancing capsule were reliable factors for the diagnosis of HCC. The formation of capsule may be related to the swelling growth of tumor, which is more common in malignant tumors with fast growth.[23] Capsule

Figure 3 52-year-old man with cirrhosis and HCC. Figure (**a**) shows APHE of Gd-EOB-DTPA MRI. Figure (**b**) shows no washout and no capsule in PVP of Gd-EOB-DTPA MRI. Tumor diameter > 2cm, and LR-4. Figure (**c**) shows washout and enhancing capsule in delayed phase of CT. Adding CT delayed-phase images to Gd-EOB-DTPA MRI, the lesion was classified as LR-5.

appearance is helpful for the diagnosis of HCC and an important index of prognosis.[24,25] Washout is related to the blood supply of HCC.[26,27] Typical HCC is supplied by arteries without portal vein blood supply, and contrast agent washout during the PVP. Washout and enhancing capsule are characteristic imaging findings of HCC, which are included as major features in LI-RADS. None of the auxiliary features were independent risk factors for the diagnosis of HCC in our study. Vender et al found that although ancillary features were an important component of LI-RADS, their impact may be small, several ancillary features likely can be removed from LI-RADS without compromising diagnostic performance.[28] It may also be the relatively small number of samples that led to our negative results, and the value of auxiliary features needs further study.

During the development of HCC, as the malignancy of the tumor increases, the normal arterial blood supply to the tumor decreases in the early stage, then the portal vein blood supply decreases, and finally the blood supply is mainly from the tumor artery.[29] In the results of our study, 4 patients with HCC showed washout in the delayed phase rather than in PVP, which we thought was due to the presence of portal venous blood supply in these tumors. According to previous studies,[30,31] the degree of histological differentiation is related to whether the tumor is washout or not and the time of washout. Recent study has found that the frequency of washout appearance was higher on CT than on gadoxetic acid-enhanced MRI (60.2%

Table 2 Tumor Features of LI-RADS

Variable	HCC (n = 52)	Non-HCC (n = 40)	k value	*P* value
MRI Major features				
APHE	41	30	0.926	0.424
Washout	33	6	0.780	<0.001*
Enhancing capsule	28	7	0.835	0.001*
MRI HCC-specific auxiliary features				
Non-enhancing capsule	1	0	1.000	0.565
Nodule-in-nodule architecture	4	2	0.776	0.470
Mosaic architecture	13	8	0.918	0.378
Fat in mass	7	5	0.860	0.574
Blood products in mass	5	3	0.820	0.512
CT washout	37	7	0.835	<0.001*

Note: *Values with statistical difference.
Abbreviations: LI-RADS, Liver Imaging Reporting and Data System; APHE, nonrim arterial phase hyperenhancement; HCC, hepatocellular carcinoma.

Table 3 Logistic Regression Analysis for the Diagnosis of HCC

Model	Variable	B	OR	95% CI	*P* value
Model 1					
	MRI washout	2.336	10.345	3.460–30.930	<0.001*
	Enhancing capsule	1.623	0.197	0.065–0.595	0.004*
Model 2					
	MRI and (or) CT washout	2.958	0.052	0.016–0.172	<0.001*
	Enhancing capsule	2.024	0.132	0.139–0.449	0.001*

Note: *Values with statistical difference.
Abbreviations: HCC, hepatocellular carcinoma; CI, confidence interval.

vs 44.3%).[32] Another study showed that the washout rate of extracellular contrast agents was 79.8% on MRI, 74.2% on CT, and 73.4% on hepatobiliary agents.[33] These results indicate that different examinations and contrast agents may affect the evaluation of tumor washout. Our results also suggest that delayed-phase CT images can detect some tumor washout that is

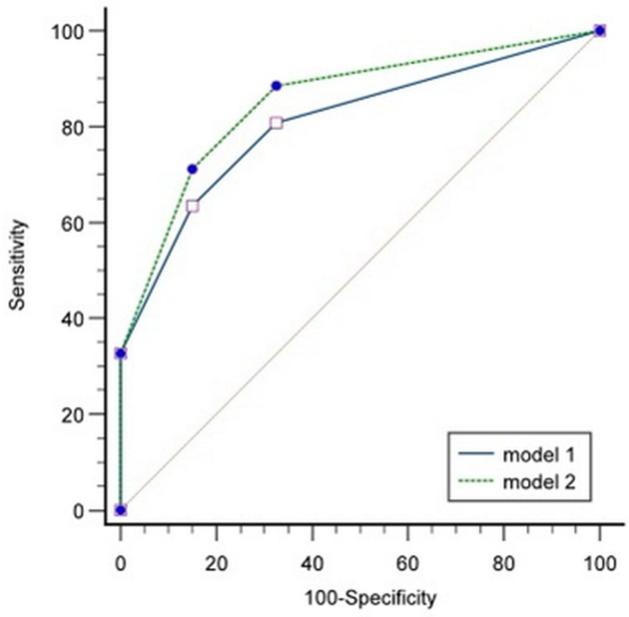

Figure 4 The blue solid line was the ROC of model 1. The green dotted line is the ROC of model 2.

not visible in PVP of Gd-EOB-DTPA to upgrade the tumor. Adding delayed CT images based on LI-RADS Gd-EOB-DTPA MRI can improve the sensitivity (71.20 vs 63.46) and the diagnostic efficiency (0.854 vs 0.808) of HCC while maintaining high specificity (85.00 vs 85.00). Therefore, we believe that CT delayed-phase images and Gd-EOB-DTPA MRI may be integrated into a single accepted diagnostic algorithm to improve diagnostic performance based on LI-RADS.

This study has several limitations. First, it is a retrospective study in a single-center, with a relatively small number of patients. A larger prospective multicenter study is needed for further external validation to reinforce our finding. Second, some of non-HCC were obtained through follow-up for more than 2 years, which is an inevitable limitation because subsequent follow-up is generally favored at this stage, rather than pathological diagnosis. Finally, the generalizability of our findings may be limited because the majority of patients had hepatitis B viral infection, and further investigation included various etiologies is required.

In conclusion, washout and enhancing capsule are reliable factors for the diagnosis of HCC. Although the LI-RADS lexicon does not permit the interchange or combined use of image modalities, the addition of delayed CT images to Gd-EOB-DTPA MRI for defining washout can improve the sensitivity of HCC diagnosis in LR-3/4 lesions while maintaining high specificity. CT delayed phase images and Gd-EOB-DTPA MRI may be integrated into a single accepted diagnostic algorithm to improve diagnostic performance based on LI-RADS. Future studies are required to reinforce our finding.

Data Sharing Statement

The data that support the findings of this study are available from the corresponding author upon reasonable request.

Author Contributions

All authors made a significant contribution to the work reported, whether that is in the conception, study design, execution, acquisition of data, analysis and interpretation, or in all these areas; took part in drafting, revising or critically reviewing the article; gave final approval of the version to be published; have agreed on the journal to which the article has been submitted; and agree to be accountable for all aspects of the work.

Funding

There is no funding to report.

Disclosure

The authors declare that there is no conflict of interest regarding the publication of this article.

References

1. McGlynn KA, Petrick JL, El-Serag HB. Epidemiology of hepatocellular carcinoma. *Hepatology*. 2021;73(Suppl 1):4–13. doi:10.1002/hep.31288
2. Zhang CH, Cheng Y, Zhang S, et al. Changing epidemiology of hepatocellular carcinoma in Asia. *Liver Int*. 2022;42(9):2029–2041. doi:10.1111/liv.15251
3. Sperber A, Bangdiwala S, Drossman D, et al. Worldwide prevalence and burden of functional gastrointestinal disorders, results of Rome Foundation Global Study. *Gastroenterology*. 2021;160(1):99–114.e3. doi:10.1053/j.gastro.2020.04.014
4. Marrero JA, Kulik LM, Sirlin CB, et al. Diagnosis, staging, and management of hepatocellular carcinoma: 2018 practice guidance by the American Association for the study of liver diseases. *Hepatology*. 2018;68(2):723–750. doi:10.1002/hep.29913
5. Tang A, Singal AG, Mitchell DG, et al. Introduction to the liver imaging reporting and data system for hepatocellular carcinoma. *Clin Gastroenterol Hepatol*. 2019;17(7):1228–1238. doi:10.1016/j.cgh.2018.10.014
6. Kanmaniraja D, Dellacerra G, Holder J, et al. Liver imaging reporting and data system (LI-RADS) v2018: review of the CT/MRI diagnostic categories. *Can Assoc Radiol J*. 2021;72(1):142–149. doi:10.1177/0846537119888393
7. Kang JH, Choi SH, Byun JH, et al. Ancillary features in the liver imaging reporting and data system: how to improve diagnosis of hepatocellular carcinoma ≤3 cm on magnetic resonance imaging. *Eur Radiol*. 2020;30(5):2881–2889. doi:10.1007/s00330-019-06645-3
8. Agnello F, Albano D, Sparacia G, et al. Outcome of LR-3 and LR-4 observations without arterial phase hyperenhancement at Gd-EOB-DTPA-enhanced MRI follow-up. *Clin Imaging*. 2020;68:169–174. doi:10.1016/j.clinimag.2020.08.003
9. Vernuccio F, Cannella R, Choudhury KR, et al. Hepatobiliary phase hypointensity predicts progression to hepatocellular carcinoma for intermediate-high risk observations, but not time to progression. *Eur J Radiol*. 2020;128:109018. doi:10.1016/j.ejrad.2020.109018
10. Zech CJ, Ba-Ssalamah A, Berg T, et al. Consensus report from the 8th international forum for liver magnetic resonance imaging. *Eur Radiol*. 2020;30(1):370–382. doi:10.1007/s00330-019-06369-4
11. Murakami T, Sofue K, Hori M. Diagnosis of hepatocellular carcinoma using Gd-EOB-DTPA MR imaging. *Magn Reson Med Sci*. 2022;21(1):168–181. doi:10.2463/mrms.rev.2021-0031

12. American College of Radiology. LI-RADS version 2018. Available from: https://www.acr.org/Clinical-Resources/Reporting-and-DataSystems/LI-RADS/CT-MRI-LI-RADS-v2018. Accessed June 6, 2023.
13. Baek KA, Kim SS, Shin HC, et al. Gadoxetic acid-enhanced MRI for diagnosis of hepatocellular carcinoma in patients with chronic liver disease: can hypointensity on the late portal venous phase be used as an alternative to washout? *Abdom Radiol*. 2020;45(9):2705–2716. doi:10.1007/s00261-020-02553-z
14. Song JS, Choi EJ, Hwang SB, et al. LI-RADS v2014 categorization of hepatocellular carcinoma: intraindividual comparison between gadopentetate dimeglumine-enhanced MRI and gadoxetic acid-enhanced MRI. *Eur Radiol*. 2019;29(1):401–410. doi:10.1007/s00330-018-5559-z
15. Joo I, Kim H, Lee JM. Cancer stem cells in primary liver cancers: pathological concepts and imaging findings. *Korean J Radiol*. 2015;16(1):50–68. doi:10.3348/kjr.2015.16.1.50
16. Kim DH, Choi SH, Kim SY, et al. Gadoxetic acid-enhanced MRI of hepatocellular carcinoma: value of washout in transitional and hepatobiliary phases. *Radiology*. 2019;291(3):651–657. doi:10.1148/radiol.2019182587
17. Kim TH, Kim SY, Tang A, et al. Comparison of international guidelines for noninvasive diagnosis of hepatocellular carcinoma: 2018 update. *Clin Mol Hepatol*. 2019;25(3):245–263. doi:10.3350/cmh.2018.0090
18. Allen BC, Ho LM, Jaffe TA, et al. Comparison of visualization rates of li-rads version 2014 major features with iv gadobenate dimeglumine or gadoxetate disodium in patients at risk for hepatocellular carcinoma. *AJR Am J Roentgenol*. 2018;210:1266–1272. doi:10.2214/AJR.17.18981
19. Jiang H, Song B, Qin Y, et al. Data-driven modification of the LI-RADS major feature system on gadoxetate disodium-enhanced MRI: toward better sensitivity and simplicity. *J Magn Reson Imaging*. 2022;55(2):493–506. doi:10.1002/jmri.27824
20. Cha DI, Choi GS, Kim YK, et al. Extracellular contrast-enhanced MRI with diffusion-weighted imaging for HCC diagnosis: prospective comparison with gadoxetic acid using LI-RADS. *Eur Radiol*. 2020;30(7):3723–3734. doi:10.1007/s00330-020-06753-5
21. Cerny M, Bergeron C, Billiard JS, et al. LI-RADS for MR imaging diagnosis of hepatocellular carcinoma: performance of major and ancillary features. *Radiology*. 2018;288(1):118–128. doi:10.1148/radiol.2018171678
22. Kierans AS, Makkar J, Guniganti P, et al. Validation of liver imaging reporting and data system 2017 (LI-RADS) criteria for imaging diagnosis of hepatocellular carcinoma. *J Magn Reson Imaging*. 2019;49(7):e205–e215. doi:10.1002/jmri.26329
23. Ishigami K, Yoshimitsu K, Nishihara Y, et al. Hepatocellular carcinoma with a pseudocapsule on gadolinium-enhanced MR images: correlation with histopathologic findings. *Radiology*. 2009;250(2):435–443. doi:10.1148/radiol.2501071702
24. An C, Rhee H, Han K, et al. Added value of smooth hypointense rim in the hepatobiliary phase of gadoxetic acid-enhanced MRI in identifying tumour capsule and diagnosing hepatocellular carcinoma. *Eur Radiol*. 2017;27(6):2610–2618. doi:10.1007/s00330-016-4634-6
25. Chong HH, Yang L, Sheng RF, et al. Multi-scale and multi-parametric radiomics of gadoxetate disodium-enhanced MRI predicts microvascular invasion and outcome in patients with solitary hepatocellular carcinoma ≤ 5 cm. *Eur Radiol*. 2021;31(7):4824–4838. doi:10.1007/s00330-020-07601-2
26. Ayuso C, Rimola J, Vilana R, et al. Diagnosis and staging of hepatocellular carcinoma (HCC): current guidelines. *Eur J Radiol*. 2018;101:72–81. doi:10.1016/j.ejrad.2018.01.025
27. Choi BI, Lee JM, Kim TK, et al. Diagnosing borderline hepatic nodules in hepatocarcinogenesis: imaging performance. *AJR Am J Roentgenol*. 2015;205(1):10–21. doi:10.2214/AJR.14.12655
28. Vander Pol CB, Dhindsa K, Shergill R, et al. MRI LI-RADS version 2018: impact of and reduction in ancillary features. *AJR Am J Roentgenol*. 2021;216(4):935–942. doi:10.2214/AJR.20.23031
29. Narsinh KH, Cui J, Papadatos D, et al. Hepatocarcinogenesis and LI-RADS. *Abdom Radiol*. 2018;43(1):158–168. doi:10.1007/s00261-017-1409-8
30. Jang HJ, Kim TK, Burns PN, et al. Enhancement patterns of hepatocellular carcinoma at contrast-enhanced US: comparison with histologic differentiation. *Radiology*. 2007;244(3):898–906. doi:10.1148/radiol.2443061520
31. Okamoto D, Yoshimitsu K, Nishie A, et al. Enhancement pattern analysis of hypervascular hepatocellular carcinoma on dynamic MR imaging with histopathological correlation: validity of portal phase imaging for predicting tumor grade. *Eur J Radiol*. 2012;81(6):1116–1121. doi:10.1016/j.ejrad.2011.02.056
32. Nakao S, Tanabe M, Okada M, et al. Liver imaging reporting and data system (LI-RADS) v2018: comparison between computed tomography and gadoxetic acid-enhanced magnetic resonance imaging. *Jpn J Radiol*. 2019;37(9):651–659. doi:10.1007/s11604-019-00855-x
33. Min JH, Kim JM, Kim YK, et al. Magnetic resonance imaging with extracellular contrast detects hepatocellular carcinoma with greater accuracy than with gadoxetic acid or computed tomography. *Clin Gastroenterol Hepatol*. 2020;18(9):2091–2100.e7. doi:10.1016/j.cgh.2019.12.010